OIS.360 - Accuracy and reconstruction quality of an innovative oblique imaging system:

Gerhard Kemper[1]

Summary

Oblique camera technology has been used in aerial surveys with airplanes for 15 years and, meanwhile, also with UAVs. The demand for data for 3D reconstruction of buildings is high. The innovative camera system OIS.360 represents a significant innovation in the market by eliminating the need for cost-intensive hardware. Demonstrating the accuracy and reconstruction quality is the subject of this work. An increased number of captured perspectives contrasts with potential mechanical instability, limits in GSD, and insufficient overlaps. However, capturing 8 perspectives surpasses conventional systems. This article deals with calibration and reconstruction workflows and examines whether sequentially acquired data are comparable to conventional systems. Different evaluation sequences are compared in order to analyze AT results, camera calibration, and the repeatability of the angles derived solely from GNSS measurements. A comparison of reconstruction quality using Gaussian splatting is also carried out in this study.

Keywords: oblique imaging system, digital twin, Gaussian splatting, camera calibration

1 Sensor system

Compared to systems with 5 cameras (nadir plus 4 oblique cameras), OIS.360 uses one nadir and one rotating oblique camera with 120 MP and global shutter technology.

1
S

Figure 1: OIS.360 during a mechanical stress test in the laboratory with more than 250,000 cycles.

The advantage lies in the significantly reduced acquisition cost (-60%) and in the ability to capture eight perspectives with a rotation of 45° and a tilt angle of 45°. The images are captured sequentially, producing eight frames within three seconds. This can lead to less overlap along-track but to more views and greater overlap across the entire block. Since the camera rotates back to its initial position, there is a period of about 400 ms during which no images can be taken, which, depending on flight speed, limits the maximum GSD and the corresponding overlap.

1.1 System description

As the nadir camera, a 150 MP medium-format camera with a 70 mm lens is integrated. It is triggered in the conventional way via a flight navigation software after prior flight mission planning (overlap, GSD, terrain following) using the GNSS position. For the oblique image planning, additional flight strips and strip lengths are required in order to sufficiently cover the planned area with the oblique camera.

The oblique camera is a PhaseOne iXM-GS 120 with an 80 mm lens. It is mounted on a rotary bearing and precisely controlled via a stepper motor. At its core is a highly integrated stepper motor controller with an encoder, operated via low-level firmware.

Acceleration, deceleration, triggering, capturing the camera signal, and re-acceleration present the complex challenge of avoiding vibrations upon stopping and ensuring the camera is 100% statically at rest during exposure. This compromise between fast sequencing and sharp image capture is the centerpiece of the development, requiring extensive programming of acceleration and deceleration ramps to prevent oversteering, step losses, and post-oscillation of the unit. An optimal center of gravity is essential, necessitating precise mechanical construction.

Power supply, image data transfer, and control of trigger and event signals as well as GNSS tags are handled via cable feeds, requiring the camera to rotate back to the starting position at the end of the sequence. Eight exposures are triggered at 325 ms intervals, with about 900 ms needed for the return trip (315°).

Processing the image data at this fast frame rate (up to 5 fps) is only possible with a proprietary software solution. This also allows setting aperture, shutter speed, and ISO, as well as preview images. The data is captured in compressed

IIQs format, which can be directly processed by various programs. The image sequence is started at the beginning of the flight line and repeated at maximum speed until the end of the line.

Figure 2. Static footprints at 6 cm GSD for the OIS.360

1.2 Testflight

In the fall of 2025, a total of three flights were conducted with Geoplana GmbH.

On September 18, the first test flight over Marbach was carried out using a still-modified camera-lens combination to fundamentally validate the concept. It turned out that the 110 mm Schneider lens was not ideal for the oblique camera, as the line resolution was insufficient for the sensor, resulting in slight blurriness.

Another flight over Schwäbisch Hall on November 13 with the new sensor and lens combination delivered optimal results in image quality, however s with problems in image storage with the new Capture Software in combination with flight guidance.

A third flight on December 1st over Marbach was able to resolve the issues with the overall control. Angle calculations were also introduced into the Geo-Tags, based purely on GNSS data. These will later be compared and discussed with the AT results.

The missions were planned for 4 cm GSD for the nadir camera with 80/60% overlap. This is a very common configuration for oblique missions. This resulted in an average GSD of 5 cm for the oblique views. Planned and navigated with Topoflight, position and rotation parameters are stored in a log file as well as in the Exif information.

In the last flight, some strips were flown with a nadir GSD of 3 cm to improve camera calibration and as an attempt to achieve higher resolutions beyond the planned specification.

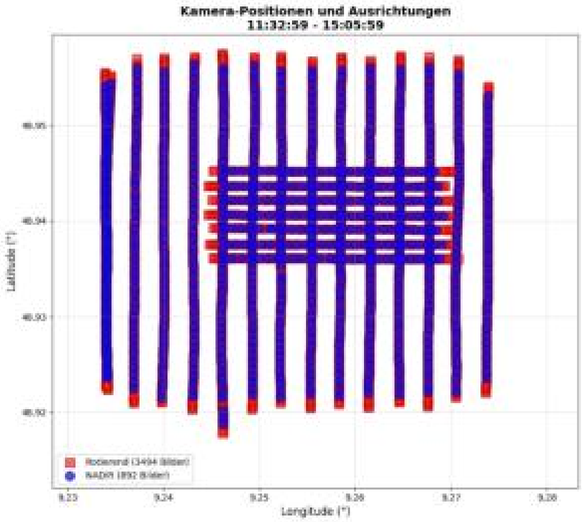

Figure 3. Result of the aerial survey on 1 December with 3 and 4 cm GSD over Marbach

2 Aerotriangulation

The image data processing was carried out in various programs such as Skyline PhotoMeshTM and Agisoft Metashape, as well as Bingo. While PhotoMeshTM can work directly with the internal IIQ format, the images had to be converted to TIFF for the other programs.

All programs were able to tie the images together without issues and deliver good AT results. The speed of the tie-point matching was highly dependent on the quality of the supplied EO data. In the last flight, which also provided approximate angles, the tie-point matching and AT process was about 60% faster, especially in PhotoMesh.

Figure 4 Sequential image sequence from the oblique camera

2.1 AT of various image sequences

In the following, specific combinations of image perspectives were selected to be oriented separately. Overall, Photomesh and Bingo achieved better and more robust results. All variants went through the same process path to compare image linking, camera calibration and AT.

A setup similar to standard oblique camera systems was selected with 4 oblique views (rear, front, left, right) plus nadir view. An overall accuracy of 0.4 pixels was achieved, which is actually comparable to previously tested classic systems (e.g. OIS.L) [3].

In a second scenario, the four image views diagonal to the nadir camera at 45 degrees (left rear, left front, right front, right rear) plus the nadir view were used. Here, too, a comparable accuracy of 0.4 pixels was achieved, although an improvement was expected due to the changed perspective and the different matching pattern.

The use of all 8 oblique views without nadir images results in an accuracy of 0.65 pixels for the entire image block, which is lower than the classic system. This is understandable, as a nadir camera offers independent resolution and observations, which enables independent correction of the entire block.

By accepting reduced geometric accuracy, it would be possible to dispense with a camera.

As expected, using all 8 views plus the nadir camera delivered the best result with approximately 0.32 pixels and very robust camera calibration.

The advantage of the OIS.360 is that it only contains 2 camera heads, meaning that only 2 internal orientations (camera calibrations) need to be determined. A classic system has more degrees of freedom here and is geometrically less stable. Nevertheless, the accuracy is not significantly higher, which is reflected in the somewhat indeterminate image overlap and image sequence and thus greater variability of the EO.

2.2 Camera calibration

The results of the camera calibration varied slightly depending on the software and image sequence. The camera calibration was determined based on the flight data. Control points were not used for this test. When evaluating only the oblique images, Metashape calculated larger differences between the calibrated focal length and the factory calibration; this was solved much better by Photomesh and Bingo.

In the Schwäbisch Hall aerial survey, where there are significant differences in elevation between the terrain and buildings, all programmes performed adequately well and were close to the factory calibration. In the last aerial survey over Marbach, where 7 additional flight strips were captured at 3 cm GSD, Metashape also achieved good calibration of all parameters, including the focal length. 4075 images were included in the calculation.

The resulting residual distortions no longer showed any systematic patterns, indicating successful calibration. These correspond to classic systems with multiple cameras [2, 3] but also to individual medium-format cameras [4].

	Value	Error	F	Cx	Cy	B1	B2	K1	K2	K3	K4	P1	P2
F	23336.3	4.45606	1.00	-0.05	0.18	-0.29	-0.03	-0.99	0.98	-0.93	0.92	-0.05	0.19
Cx	51.295	4.10289		1.00	-0.02	0.05	0.70	0.05	-0.05	0.06	-0.06	1.00	-0.02
Cy	570.068	3.15858			1.00	-0.45	0.02	-0.15	0.14	-0.13	0.12	-0.02	0.99
B1	-116.211	0.229329				1.00	0.01	0.29	-0.30	0.30	-0.29	0.05	-0.44
B2	4.35067	0.171878					1.00	0.03	-0.04	0.04	-0.04	0.71	0.02
K1	0.0522972	0.0106385						1.00	-0.99	0.98	-0.95	0.05	-0.16
K2	0.132036	0.21498							1.00	-0.99	0.98	-0.05	0.16
K3	-0.629283	1.07828								1.00	-0.99	0.06	-0.15
K4	7.30619	6.02382									1.00	-0.06	0.14
P1	-1.54201e-05	0.0001105084										1.00	-0.02
P2	0.00139071	7.99997e-05											1.00

Figure 5: Calibration matrix for the oblique camera

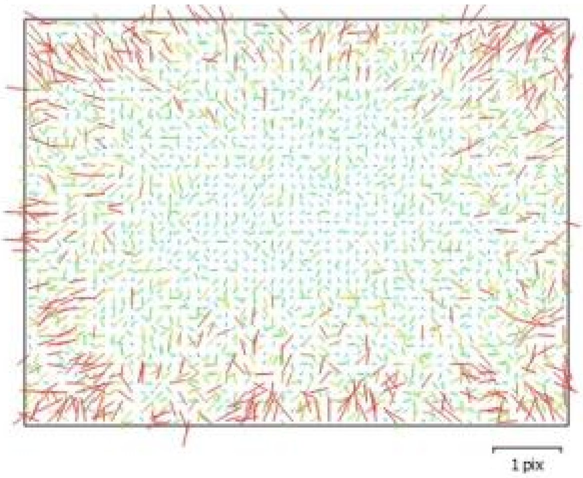

Figure 6 : Residual error plot of the oblique camera

2.3 Start-Parameter / Geotags

A GNSS receiver was already integrated in the last flight, and its values, including the calculated angles, were written into the EXIF data of the images. The pitch and roll angles were set to 0 for the nadir camera, and the heading angle was calculated from the ground track of the GNSS data. This is only a rough estimate, but it helps to sort the images roughly. For the oblique camera, the pitch was set to the mounting angle of 4 degrees, the roll angle to 0 degrees, and the heading angle was calculated from the ground track using the increment values of the motor sensor. Again, this is only a rough assumption, but it helped Photomesh to perform image linking and AT in 50% of the time.

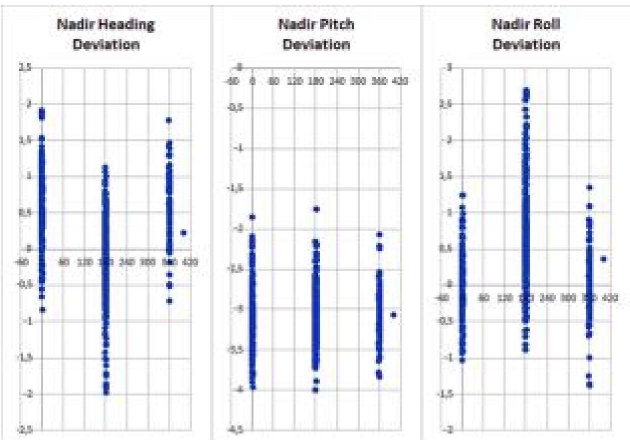

Figure 7 : Deviation between target and AT values

Figure 7 shows systematic deviations of the calculated AT angles depending on the flight direction. In addition to the variation in the heading angle of approximately +-1.5°, a drift due to crosswind can be observed in the flight direction. The offset amounts change with the flight direction. This does not occur with the nadir deviation of pitch; instead, there is a constant slanted installation position of approximately -3.2°. The fluctuation is unspecific at approximately +- 1°. With the roll movement, there is a variation of +- 1° with a slight dependence on the flight direction or crosswind. A slight improvement could be achieved by calibrating the installation position. A GNSS IMU solution is possible, at least for the nadir camera.

It is not possible to install an IMU on the rotating camera, as the acceleration would not provide reliable values without suitable Kalman filters and the use of special weighting of the individual sensors. Figure 8 shows the same analysis on the oblique camera.

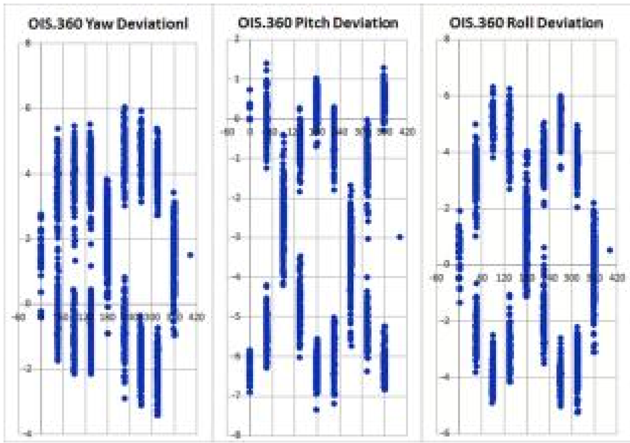

Figure 8: Same analysis on the oblique camera.

The picture is actually similar to that of the nadir camera. However, the camera rotates against the direction of flight and the calculated heading causes a fluctuation range of +-1.5° on the Y-axis from the ‘course over ground’ values. The direction of flight now also comes into play with the pitch variance. The basic deviation of -3° jumps with the heading of the camera and the fluctuation range moves on the y-axis. The same can be observed for the roll angles; here, too, there are systematic deviations with the viewing or flight direction.

2.4 Concepts for improving EO parameters

The systematic errors show that there is room for improvement. Systematics can be calculated in advance or calibrated. For example, the systematic deviations of the nadir camera, which reveal mounting errors, could be used to correct the pitch angle by 3° and the heading and roll by approximately 0.3°. Dynamic errors caused by flight movement cannot be corrected. In this flight, these show a fluctuation range of +-1.5° in heading and a direction-dependent offset of 3°.

The goal now is to integrate a smaller GNSS-IMU unit on the nadir camera, which can determine the rotation angle to 0.2°. Once this GNSS-INS solution has been calibrated to the nadir camera [1], the next step is to calibrate the oblique camera to the nadir camera, taking into account the constantly changing reference systems. However, this requires good mechanical reproducibility of the recording positions. This is achieved electromechanically to less than 0.1° thanks to the resolution of the stepper motor, the incremental encoder and the reduction gear. Step errors are always detected and corrected. This was optically verified using slow-motion video recordings with measuring marks on the turntable and bearing mount, which allows a resolution of better than 0.5°. With this modification, the system can be improved with GNSS-INS, thus providing better input parameters and reducing control points.

3 3D Reconstrution

Various approaches were also chosen for the 3D reconstruction in order to examine the options offered by different setups. All images had the problem of long shadows due to the season and, overall, low light but high contrast. Here, Photomesh was able to utilise the full bit width of the digital images by directly using the IIQ format, thus achieving a good representation of the shadow areas next to the sometimes very bright facades. Model generation was performed for all three flights using Skyline Photomesh.

The evaluation of flight 1 of the eight oblique aerial images also yields good results on the ground, but with slightly lower sharpness on the facades and edge structures. Geometric accuracy also appears to suffer somewhat at edges and ridges as well as ground structures. This means that the use of a single camera with 8 views leads to excellent results in the 3D construction of buildings, but the accuracy of the overall image block lags behind the accuracy of classic systems. The additional use of nadir images provides a better representation of the ground between buildings and also of edges, which can certainly be attributed to the improved geometry. However, the poorer optics of the oblique camera in this flight also play a role, making the model of pure oblique views appear softer.

Figure 9-10 : Above: Marbach city centre generated using only oblique images; below: with the addition of the nadir camera

3.1 Auswertung Schwäbisch Hall

During the flight over Schwäbisch Hall, an almost perfect model was generated from the image data. During this flight, there were problems between the image memory and flight control, which led to non-homogeneous flight lines, individual image errors and a few overlap losses. In addition, the lighting conditions in the narrow Kocher valley were quite problematic. Here, the use of raw image data was able to compensate for many issues and also enable good resolution in the shadows.

The dynamics of the cameras in particular can still deliver flawless results in raw format, which is unexpected at this time of year. An initial analysis of the data shows in the following figures the extremely high contrast of the overall model and the still recognisable structure in the deepest shadows of the model.

Figure 11 : low November sun with almost black areas behind the steep wall of the Kocher

Figure 12 : Drawing in the almost black area thanks to raw image format IIQ

3.2 Gaussian Splatting

A Gaussian splatting experiment with photomesh was carried out using the first flight over Marbach and the second flight over Schwäbisch Hall.

Gaussian splatting analyses surfaces and their relationship to neighbouring points. This works best with as many perspectives as possible and can thus better represent solitary objects such as masts, scaffolding or other free-standing or solitary structures.

Even at the edges of buildings, the representation is often better than models generated solely from 3D meshes. In contrast, when viewed very closely, surfaces often appear slightly blurred. However, the details of the scaffolding, as well as the facades and roof edges, are significantly better.

Figure 13-14: Above: the result of normal processing; below: using Gaussian splatting from 8 perspectives

The following images of Grosscomburg Monastery near Schwäbisch Hall were created using the recently released beta version of Photomesh with improved use of IIQ data and optimised Splat function.

The overall image is softer in colour (more realistic) and the hard shadows have been further improved to highlight recognisable structures. The structures of the tower spires are very clearly visible in the Splat variant, as are the scaffolding and other parts of the façade. Overall, the Splat model is more vivid and sharper.

.

Figure 15 : 3D model of Grosscomburg Monastery near Schwäbisch Hall

Figure 16 : 3D model with Gaussian splatting of the Großcomburg monastery near Schwäbisch Hall

4 Discuss

The innovative new OIS.360 in its current version delivers results that are absolutely comparable to classic systems with five cameras for oblique images with a GSD of up to 5 cm. Its more compact and significantly less expensive design is an advantage for limited budgets. or for integration problems in cramped aeroplanes. The maximum possible GSD depends on the flight speed. At a maximum flight speed of 95 knots, planning for a 4 cm oblique image GSD also delivered very good results.

In comparison to AT accuracy and camera calibration, the OIS.360 is comparable to classical system.

With the tested programmes, all test flights were well balanced, but other systems seem to require more accurate input or start values to solve the AT. These are not yet provided well enough in the current version (see chapter Outlook).

In fact, in these tests and the flown resolutions of 5 cm through the 8 perspectives, a slight advantage in reconstruction behaviour with regard to Gaussian splatting can be observed. The overlap gap when turning the cameras back did not show any noticeable loss of quality in any of the models, at least not at a GSD of up to 5 cm.

5 Outlook

The OIS.360 is currently being tested for real-world operation, including endurance testing of the bearings and final integration of an IMU to generate better start values. Integration of a GNSS with 2 cm resolution is available as an option. The current accuracy of 1 m with 0.5 degrees of angle is already significantly better than the solution used in the test flights in autumn 2025. Optimisation of the image capture software, flight control and operator interface has already been implemented. The system will be ready for production in February and available for delivery in March.

Work is already underway on a faster rotation technology. Initial tests with other motor stages, gear ratios, control algorithms and slightly more powerful motors have made it possible to reduce a full cycle to up to 2 seconds. This also enables higher resolutions (smaller GSD) with sufficient overlap or, with the same GSD, more data for improved 3D reconstruction. This means that the system scales down in terms of time in the recording cycle, and the gap for turning back also becomes smaller, but is still present.

Therefore, experiments with slip rings are planned, whereby the difficulty of the high data volume is only possible via fibre optic transmission. At the same time, power and signal data must also be looped. If this were to succeed, the limiting factor would be the camera's frame rate of 4-5 fps and a full cycle of 1.6 seconds, making a GSD of 2.5 cm theoretically possible.

Bibliography

[1] Kemper, G., Pivnicka, F. & Geissler, S. (2012). Calibration Procedures in Mid Format Camera Setups; XXII ISPRS Congress, ISPRS Proceedings, Melbourne/ Australia.

[2] Kruck, E. & Melykuti, B.(2014). Kalibrierung von Oblique- und UAV Kameras, Jahrestagung der Deutschen Gesellschaft für Photogrammetrie, Fernerkundung und Geoinformation, Hamburg, 2014

[3] Kemper, G., Melykuti, B. & Yu, C. (2016). Calibration procedures on oblique camera setups: XXIII ISPRS Congress, ISPRS Proceedings, Commission I, WG I/1, Prague /CZ

[4] Tölg, T., Kemper, G. & Kalinski, D. (2016). Medium-format camera evaluation based on the latest PhaseOne technology; XXIII ISPRS Congress, ISPRS Proceedings, Commission I, WG I/2, Prague /CZ

Orlik, T., Schechter, E.B., & Kemper,G. (2021). 3D Modelling using aerial oblique images with close range UAV based data for single Objects. ISPRS 2021

Motz, M., Kemper, G. & Ciobanu, D. (2021). Accuracy validation of tilted camera setups in open skies project and mapping applications. ISPRS 2021

Fraser C. & Stamatopoulos C. (2014). Automated target-free camera calibration. ASPRS 2014 Annual Conference: Geospatial

Heipke, C. (2017). Photogrammetrie und Fernerkundung. Handbuch der Geodäsie, herausgegeben von W. Freeden und R. Rummel. https://doi.org/10.1007/978-3-662-47094-7